Transient ion ejection during nanocomposite thermite reactions

Lei Zhou,[1] Nicholas Piekiel,[1] Snehaunshu Chowdhury,[1] Donggeun Lee,[2] and Michael R. Zachariah[1,a)]
[1]*Department of Mechanical Engineering and Department of Chemistry and Biochemistry, University of Maryland, College Park, Maryland 20742, USA*
[2]*School of Mechanical Engineering, Pusan National University, 30 Jangjeon, Geumjeong, Busan 609-735, Republic of Korea*

(Received 4 June 2009; accepted 14 August 2009; published online 30 October 2009)

We observe an intense ion pulse from nanocomposite thermite reactions, which we temporally probe using a recently developed temperature jump/time of flight mass spectrometer. These ion pulses are observed to be much shorter in duration than the overall thermite reaction time. Ion ejection appears in stages as positive ions are ejected prior to nanocomposite thermite ignition, and ignition of the thermite mixtures leads to a second ionization step which is primarily dominated by negative species. The positive species are identified from mass spectrometric measurements and the results show that the positive ion species are comprised of Na ions with minor species of Al and K ions. This observation can be explained by a diffusion based ion-current mechanism, in which strong Al ion diffusion flux formed through the oxide shell, and the surface Na and K ions from salt contaminations are ejected by the strong electrostatic repulsion. The fact that the negative ionization step occurs during the ignition event suggests a strong relation between the nanocomposite thermite reaction and the negative ionization process. © *2009 American Institute of Physics*.
[doi:10.1063/1.3225907]

I. INTRODUCTION

Nanocomposite thermites, also known as metastable intermolecular composites (MICs), are comprised of reactive components consisting of nanostructured particles that are intimately mixed. The unique nanostructure of MICs not only enhance the reactivity, but also allow a control over the reactivity by varying parameters such as particle size, morphology, and local composition.[1–3]

This class of material has not been studied as extensively as traditional organic based energetic materials. Research on thermite energetic materials typically focuses on developing new thermite formulations, as well as studying the thermite reaction mechanism. In general, a thermochemical point of view is emphasized in mechanism studies by means of characterizing combustion properties such as flame speed, reaction rate, ignition temperatures, or reaction products.[4–9] On the other hand, the literature shows that complex ionization phenomena are observed through a variety of combustion systems.[10,11] Ershov studied the detonation of solid explosives such as 2,4,6-trinitrotoluene (TNT) and pentaerythritol tetranitrate (PETN), and observed high degrees of ionization in the detonation front. The corresponding electron density is several orders of magnitude higher than the theoretical value estimated from the Saha equation, which indicates nonthermal channels of ionization.[12] Experiments also revealed transient electric/magnetic field generation from combustion of a variety of metal-gas and metal-metal reaction systems, which may be attributed to the different diffusion rates of charge carriers through the oxide shell.[13–20] More recently, molecular dynamic simulations show that strong electric fields are intrinsically formed across the oxide shell of aluminum nanoparticles.[21] In fact, the electrical fields can be considered as inherent reaction parameter which should be accounted for in a model for thermite initiation or potentially be used as a controlling parameter though application of external fields.[22,23]

The above experimental and theoretical investigations suggest an incomplete understanding of the origin of this behavior and if indeed it could be manipulated. Only a few studies report on ionization phenomena in nanocomposite thermites. Douglas *et al.*[24] took a similar approach to Ershov's work and studied the electrical conductivity induced by nanocomposite thermite reactions. Their work showed that a conduction zone was observed in the reaction front and that the conductivity profile was much longer than organic high explosives. Korogodov *et al.*[25] measured microwave radiation pulses from the combustion of an Al/Fe_2O_3 nanocomposite thermite system to be several orders of magnitude higher than thermal radiation.

Recently we reported on the development of a "temperature-jump/time-of-flight mass spectrometer" (T-Jump/TOFMS) that is capable of monitoring the transient reaction of organic based energetic materials [e.g., hexahydro-1,3,5-trinitro-1,3,5-triazine (RDX), nitrocellulose, etc.].[4] However, when attempting to conduct experiments with nanothermites, we found that initiation of the exothermic reaction caused a catastrophic malfunction of the high voltage bias on the ion extraction optics and resulted in loss of mass spectra signal. This observation leads us to realize that an intense flux of charged species (ions and electrons) is ejected from the thermite reactions. Furthermore through appropriate configuration of the electric field within the mass spectrometer we have the opportunity to probe with very

a)Author to whom correspondence should be addressed. Electronic mail: mrz@umd.edu. Tel.: 301-405-4311. FAX: 301-314-9477.

high temporal resolution the nature of the current pulse and its relationship to the combustion process. Here we apply T-Jump/TOFMS with minor modifications to clarify the characteristic nature of the ionization and its temporal correspondence to nanothermite combustion.

II. EXPERIMENTAL APPROACH

Thermite composite samples were prepared by mixing aluminum nanoparticles with oxidizer particles to obtain a stoichiometric mixture. The aluminum used was 50 nm aluminum explosive powder obtained from Argonide Corporation. Four types of oxidizers, copper oxide (CuO), iron oxide (Fe_2O_3), bismuth oxide (Bi_2O_3), and tungsten oxide (WO_3), nanopowders of ~100 nm obtained from Sigma-Aldrich, were used in a mix with aluminum particles. Nanocomposite thermite samples were mixed in hexane and the suspensions were sonicated for about 30 min to break the agglomerates and ensure intrinsic mixing between the fuel and oxidizer. The prepared sample suspensions were then coated on the T-Jump probe with a dropper. The T-Jump probe is a ~10 mm long platinum wire with diameter of 76 μm, for which the center ~5 mm of the wire is coated with a thin layer of sample comprising less than 0.3 mg.

The T-Jump/TOFMS is comprised of a linear time-of-flight chamber, an electron gun ionization source, and the T-Jump probe with an electrical feedthrough for rapid sample heating. A detailed description of the T-Jump/TOF mass spectrometer can be found in our previous work.[4] In this work, different electric field configurations were used to extract ions of interest. The schematic of ion optics is shown in Fig. 1. The ion optics consist of an ion repeller plate A1, an ion extraction plate A2, and an ion acceleration plate A3. A liner system was used to ensure a field-free ion drifting region in the time-of-flight tube, and a microchannel plate (MCP) detector was used to measure the extracted ions. Since the primary interest in this study is to probe the intrinsic ions generated by the thermite event, the electron impact ionization source was not used for most of the experiments. The four experimental configurations of ion optics voltages and probe positions are summarized in Table I.

The ion pulse was measured by inserting the T-Jump probe between the repeller plate A1 and the extraction plate A2 as shown in Fig. 1. Charged species were continuously extracted by the ion optics and, consequently, the ion signal detected from the MCP is proportional to the total number of charged species generated during the thermite reaction, but does not contain any ion mass information. To obtain an ion mass we pulse the ion optics in order to determine a drift time. In this manner the T-Jump/TOFMS was operated in the same way as we illustrated in our previous work,[4,26] but without the electron impact ionization source. The T-Jump probe was placed outside, but near the ion extraction region, to obtain positive ion mass spectra. We were unable to obtain negative ion spectra due to thermite reaction induced arcing in the ion-extraction region.

In addition to the ion pulse signals and mass spectra measurements, a high speed camera system (Phantom 12.1) was used to capture the optical emission from the ignition/combustion events. The camera captures images at a rate of 30 μs per frame. For optical data processing purposes, we consider each image as a matrix of pixels, and the magnitude of the values in the matrix is the optical intensity for a given pixel, thus the total optical intensity from the summation of the matrix can be found for each image. The time resolved optical profile of each heating event can be obtained by plotting the total optical intensity versus heating time. The optical profile can be considered as a measure of the reactivity and can be directly compared with the ion signal obtained from the same ignition event.

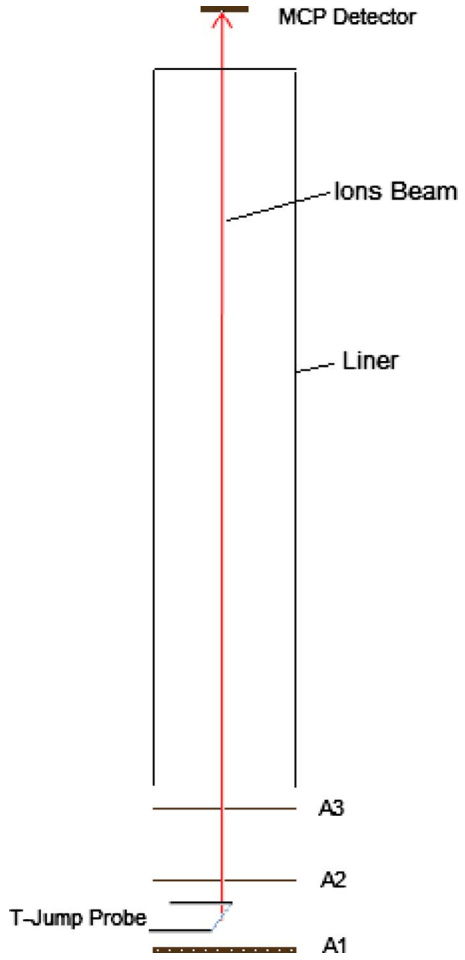

FIG. 1. (Color online) Schematic of ion optics in the T-Jump/TOFMS.

III. RESULTS AND DISCUSSION

A. Ignition behavior observed by optical emission

The ignition behavior of nanocomposite thermite samples in the T-Jump experiments was first examined from the time resolved images recorded by the high speed camera. Selected images for a Al/CuO thermite reaction are shown in Fig. 2(a) and the corresponding time resolved optical profile is presented in Fig. 2(b). The time dependent temperature trace calculated from probe resistance change is also shown in Fig. 2(b). The result shows that the temperature rises to ~1600 K in 2.7 ms, i.e., a heating rate of $\sim 5 \times 10^5$ K/s. This heating rate was used throughout our T-Jump experiments. It is seen from Fig. 2(a) that the optical registration is first observed at the two ends of the sample coating at a time

TABLE I. Summary of the configurations of ion optics voltages and probe position.

	Positive ions	Negative ions[a]	Positive mass spectra	Negative mass spectra[b]
Probe position	Inside	Inside	Outside	Outside
A1	Ground	dc −200 V	Ground	Pulsed ground to −200 V
A2	dc −200 V	Ground	Pulsed ground to −200 V	Ground
A3 and liner	dc −1500 V	dc +1300 V	dc −1500 V	dc +1300 V

[a]Al/Bi_2O_3 thermite mixture caused arcing in this configuration.
[b]All four types of thermite mixtures caused arcing in this configuration.

of 2.040 ms, indicating the ignition of the thermite sample. The ignition front then propagated from the two ends toward the center and ignited the whole thermite sample at a time of 2.187 ms. We define this ignition propagation time as the ignition interval as shown in Fig. 2(b). Quite clearly seen in Figs. 2(a) and 2(b) is that the thermite sample is also blown off the wire after the ignition and continues to react until ~3 ms, i.e., overall reaction time of ~1 ms. For the other nanocomposite thermite systems investigated, e.g., Al/Fe_2O_3, Al/WO_3, and Al/Bi_2O_3, similar ignition behavior was observed from the camera images. However, due to space limitations, we will only show the time resolved optical intensity profile in the rest of our analysis. .

B. Ion pulse generation and its relationship to ignition

Figure 3 shows typical results of the positive ion pulse signal measurement for (a) Al/CuO, (b) Al/WO_3, (c) Al/Fe_2O_3, and (d) Al/Bi_2O_3 nanocomposite thermite mixtures. The ion signals are plotted as function of T-Jump heating time. The zoom-in views are also plotted in Fig. 3 to show the fine structure of the ion signals. An important piece

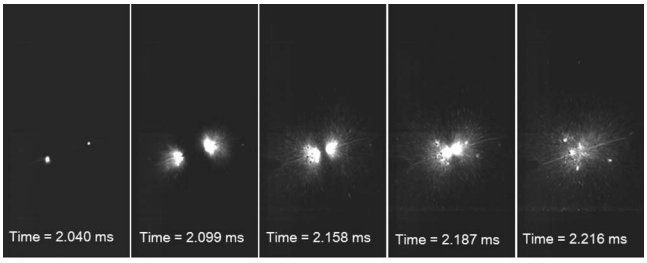

(a)

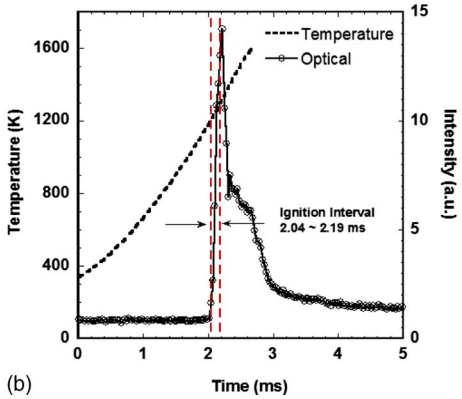

(b)

FIG. 2. (Color online) (a) Selected images for a Al/CuO thermite reaction recorded by high speed camera. (b) The time resolved optical profile of a Al/CuO thermite reaction obtained from the high speed camera images and the T-Jump temperature trace calculated from probe resistance measurement.

of information that is available from Fig. 3 is the temporal evolution of the ion generation process, which corresponds to the width of the ion signal. As we can see in the zoom-in view of Fig. 3(a), the ionization duration for Al/CuO reaction is about ~0.3 ms (from 1.85 to 2.15 ms) but the major ion pulse lasts less than ~0.1 ms, Similarly, Al/WO_3 has an ionization interval of ~0.3 ms but has an intense current spike lasting only ~0.02 ms [Fig. 3(b)]. The ion signal from Al/Fe_2O_3 reaction [Fig. 3(c)], which lasted for about ~0.4 ms, exhibits the longest ionization period among all four nanocomposite thermites. Al/Bi_2O_3 shows the shortest ionization period among all four nanocomposite thermite systems; the ion signal in Fig. 3(d) is ~0.1 ms with the major ion peak width lasting less than ~0.03 ms.

We now turn our attention to how the positive ion pulses are related to the nanocomposite thermite combustion, by comparing ion pulse signal with the corresponding time resolved optical intensity profile, which is shown at the bottom of each figure. Here we would like to first point out that although the camera and the heating of the probe are triggered simultaneously, the ions were detected by the MCP detector after the ions drifted in the linear TOF tube, so the ion signals are slightly delayed compared with the time resolved images. However, as the delay time is only of the order of ~10 μs we will ignore this difference.

As we can see from Fig. 3(a), the Al/CuO ion signal starts to rise at ~1.85 ms, much before the first ignition event at 2.04 ms was observed optically. The whole thermite sample was ignited by 2.22 ms, so that the ignition interval is 2.04–2.22 ms, and the thermite sample was continuously reacting until ~3 ms as shown in the bottom of Fig. 3(a). On the other hand, the major ion peak in Fig. 3(a) occurs at ~2.05 ms, which roughly coincides with the first ignition event, and the ion generation process is over well before the whole sample had even ignited. This behavior is particularly obvious for the Al/WO_3 system as the ion current pulse in Fig. 3(b) is complete by 2.07 ms, in contrast with the ignition which did not start until ~2.2 ms. The situation for the Al/Fe_2O_3 and Al/Bi_2O_3, Figs. 3(c) and 3(d), respectively, are not as clear. In Fig. 3(c), the positive ion pulse seems to initiate prior to ignition but the bulk of the ion generation is coincident with the ignition phase, followed by a bright emission phase that lasts well after the ion pulse is over. Finally for the Al/Bi_2O_3 system we see that optical and ion signals are coincident. These results suggest a general conclusion that the positive ion generation either precedes or is coincident with thermite initiation, and therefore is not a product of combustion but rather precedes it. Second the ion

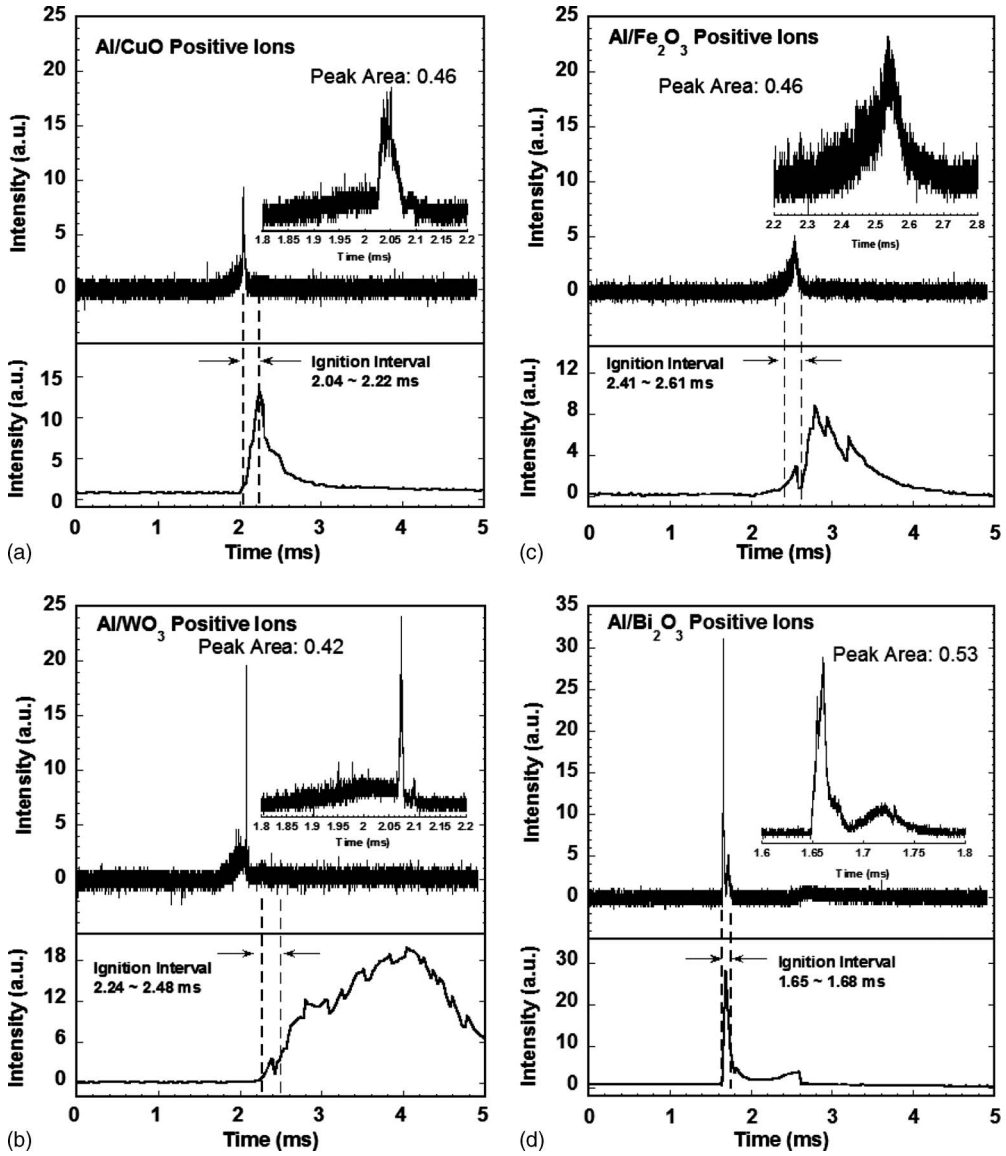

FIG. 3. Typical results of the total positive ion measurement for (a) Al/CuO, (b) Al/WO_3, (c) Al/Fe_2O_3, and (d) Al/Bi_2O_3 nanocomposite thermite mixtures. The zoom-in view shows the fine structure of the ion signal. The corresponding optical profile from the high speed camera is shown in the bottom of the each figure.

generation is relatively short, as compared to the burning time, and is relatively independent of species type.

Similar experiments were conducted to measure the negative species (ions or electrons). Figure 4 shows the negative pulse signal for (a) Al/CuO, (b) Al/WO_3, and (c) Al/Fe_2O_3, and the corresponding optical signal is also plotted at the bottom of each figure. The Al/Bi_2O_3 nanocomposite thermite reaction caused arcing for this experimental configuration and will be discussed later. In general we summarize the finding that the negative currents are longer in duration than the corresponding positive currents, but perhaps what is more intriguing is that unlike positive species which were observed before ignition, negative species were generated during the ignition, suggesting there is a separate ionization process and that the negative species were closely associated with the ignition. This suggests that there is a two step ionization process which is generic and independent of the composite formulation.

From the above temporal analysis on the positive/negative signals, we can conclude that there are two primary ionization steps around the ignition point. The first ionization step happens prior to ignition and is dominated by positive ions. Then, the ignition of the nanocomposite thermite mixture leads to a second ionization step which primarily produces negative species. After ignition has propagated along the T-Jump probe, the reactants are blown off of the wire, but the thermite reaction continues. Analysis at later times does show that there were still some ions detected during this time, but the intensity is much lower than that of the initial ion pulse.

The peak intensities of the ion peaks correspond to the instantaneous ion density and can be used as a relative measure of ionization rates. From Fig. 3, we see that ion intensity varies as a function of composite mixture, from ~5 to 30 a.u. and provides for an ordering of ionization rates: $Al/Bi_2O_3 > Al/WO_3 > Al/CuO > Al/Fe_2O_3$. Similar analysis of Fig. 4 indicates negative ionization rates are also species dependent: $Al/CuO > Al/Fe_2O_3 > Al/WO_3$.

The integrated ion signal corresponds to the total current

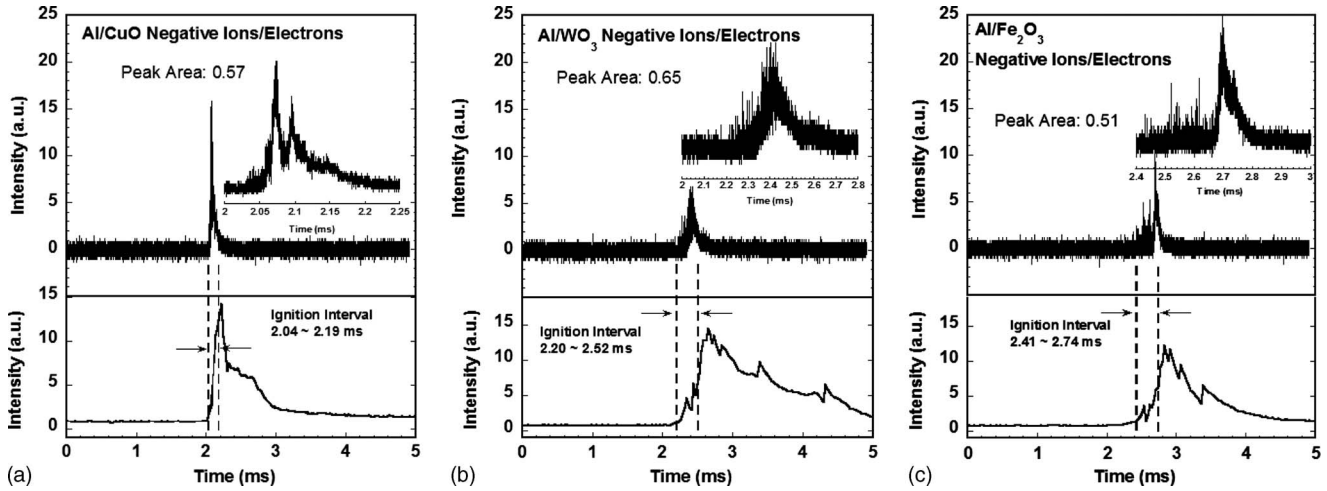

FIG. 4. Typical results of the total negative ion measurement for (a) Al/CuO, (b) Al/WO_3, and (c) Al/Fe_2O_3 nanocomposite thermite mixtures. The zoom-in view shows the fine structure of the ion signal. The corresponding optical profile from the high speed camera is shown in the bottom of the each figure.

to the detector and can be used to evaluate the overall ions densities. Figure 5 shows the integrated positive and negative currents for (a) Al/CuO, (b) Al/WO_3, (c) Al/Fe_2O_3, and (d) Al/Bi_2O_3 (only positive ion signal available). Because the positive and the negative signals are measured in separate experiments, the ignition times may be slightly different due to differences in coating thickness, wire length, etc., and one cannot directly compare the temporal evolution of the integrated curves. Nevertheless, the results for Al/Fe_2O_3 and Al/CuO systems, and especially the Al/WO_3 system, clearly show that the positive species appear before the negative ones, consistent with our temporal analysis.

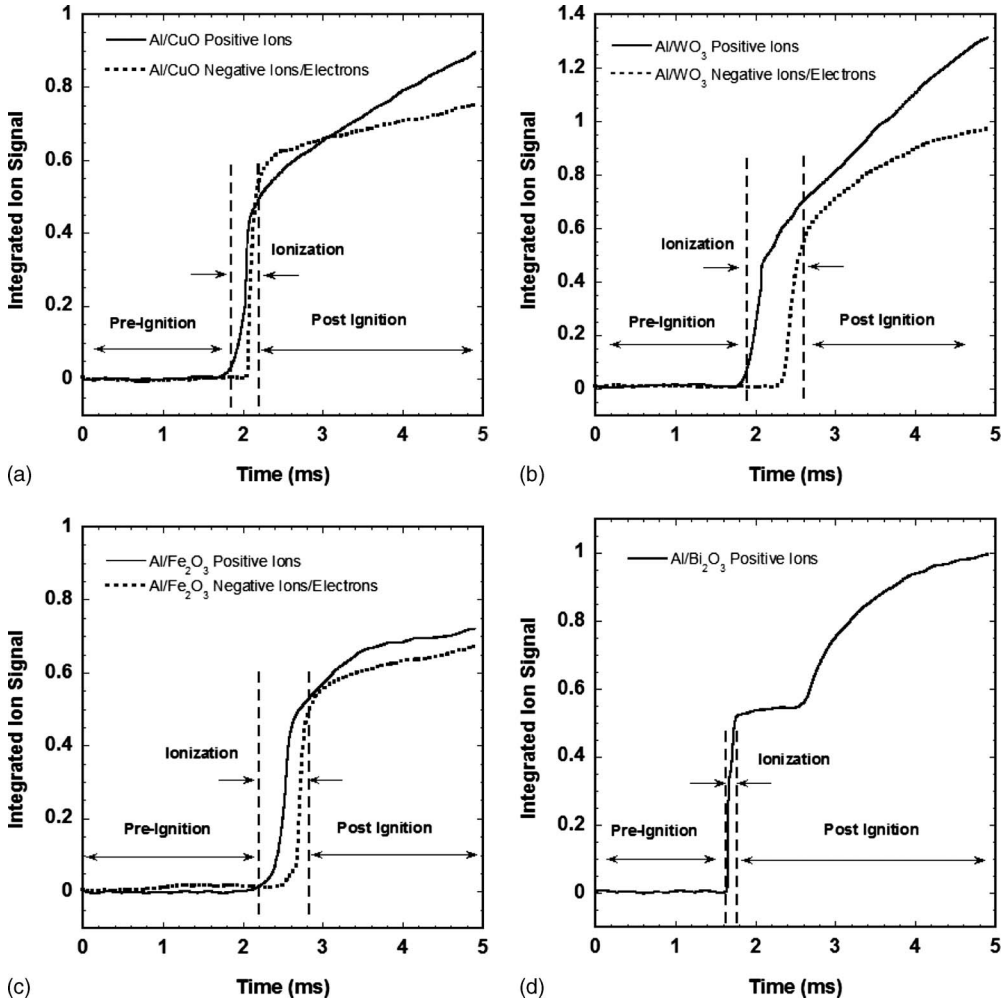

FIG. 5. The integrated positive and negative currents for (a) Al/CuO, (b) Al/WO_3, (c) Al/Fe_2O_3, and (d) Al/Bi_2O_3 (only positive ion signal available).

The integrated ion signals presented in Fig. 5 are divided into three regions labeled, preignition heating, ignition ionization (including both positive and negative ion currents), and postignition. During the initial heating, the integrated ion signals remain flat, however, as the wire is heated, both positive and negative integrated ion signals rise sharply. Following that stage, the integrated signals continuously increased, but at a much slower rate. This result indicates that there is still ion generation taking place even after the intense ion pulse is over, but with a much lower current. This is not a surprise considering the thermite powder is still reacting after the ignition interval and the chemical reaction leads to a relatively "soft" ionization. This result also indicates that the ionization through the thermochemical channels is much less intense than the ion pulse observed around the ignition interval.

In addition to the total integrated ion signals, we also calculated the peak area of the ignition associated positive/negative ion peaks, e.g., the integral of the zoom-in view signal, and the results are also listed in each of Figs. 3 and 4. The peak areas for positive ion signals are 0.46, 0.46, 0.42, and 0.53 for Al/Fe_2O_3, Al/CuO, Al/WO_3, and Al/Bi_2O_3 thermite systems, respectively. As we can see, even though the signal intensities are significantly different, peak areas observed from different nanocomposite thermite mixtures are comparable. In other words, the Al/Fe_2O_3 system ionizes at a slower rate but for longer time, while the Al/Bi_2O_3 system ionizes much more aggressively, but for a shorter duration. The result is that the overall number densities of positive ions generated from the ionization process are about the same. A similar result is also found for negative species, with peak areas for negative ion signals of 0.51, 0.57, and 0.65 for Al/Fe_2O_3, Al/CuO, and Al/WO_3 thermite systems, respectively, and consistent with the positive current results that total current generation is species independent.

Now as we compare the peak areas for the positive and negative species, we can see that there are slightly more negative species detected than the positive species. More evidence supporting a surplus of negative species can be found if we consider the fact that the T-Jump probe had a slight positively bias during heating. The presence of the T-Jump probe tends to repel the positive species but attract negative ones, so that the positive ions may be extracted with a higher efficiency than the negative species. We found that the ionization induced arcing has a polarity preference; it only occurs when we have positively biased ion optics near the T-Jump probe. Through the course of our investigation we concluded that, in general, arcing occurs if there is an open path from the T-Jump probe to a positively biased electrode. Consequently, we are not able to conduct mass spectrometry on negative species. We believe the polarity effect can be attributed to the density differences between the positive and negative ion formations. Since negative species have higher ion density than positive ones, the transient current pulse collected by the positively biased electrode is much more intense and creates a higher possibility of arcing. Furthermore, comparing with the behavior of RDX and nitrocellulose, which did not induce arcing even with positively biased ion optics,[4] we conclude that the degree of ionization from nanocomposite thermite systems is orders of magnitude higher than high explosives.

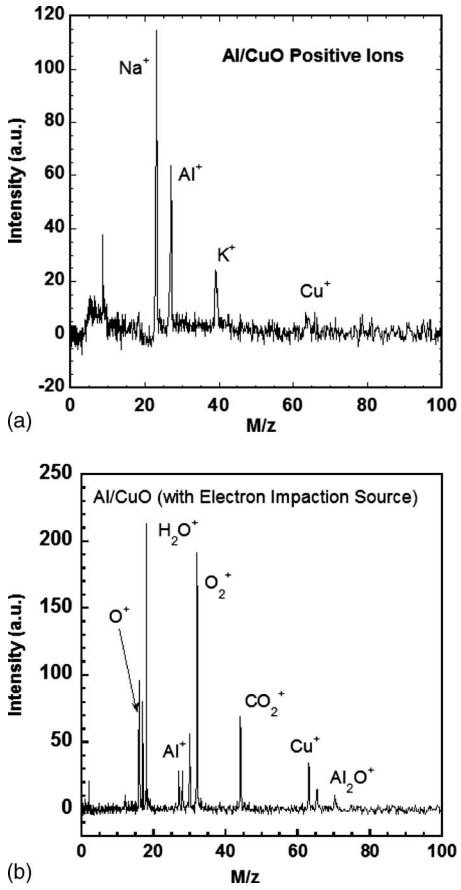

FIG. 6. (a) Example spectra for positive ion species generated from Al/CuO thermite (without external electron impact ionization source) and (b) Al/CuO thermite reaction obtained with external electron impact ionization source.

C. Species identification by mass spectrometry

Given the limitations discussed in the paragraph above regarding negative species induced arcing we turn our attention to identifying the positive ion species by mass spectrometry. The Al/Fe_2O_3 system showed relatively weak ion signal [Fig. 3(c)] and we were unable to detect any nascent ions in the TOF mass spectra. On the other hand, mass spectra for Al/CuO, Al/Bi_2O_3, and Al/WO_3 systems all show intense nascent ion signals. Example spectra for Al/CuO thermite is shown in Fig. 6(a). In these experiments the electron impact ionization source in our mass spectrometer was turned off to ensure the thermite reaction as the sole source of ions. However, the tradeoff of not using the electron gun is loss of resolution as compared to the normal mass spectrometer operation. Example mass spectra of the Al/CuO thermite reaction obtained with an external electron impact ionization source are shown in Fig. 6(b), and detailed analysis of this mass spectra can be found elsewhere.[26] Despite the lower resolution, ion peaks of Na ($m/z=23$), Al ($m/z=27$), and K ($m/z=39$) can be clearly identified in Fig. 6(a). A small peak at $m/z=64$ corresponds to Cu and suggests that Cu ions may be generated as minor species from the thermite reaction

induced ionization. Mass spectra for both Al/Bi_2O_3 and Al/WO_3 showed similar results to the Al/CuO. Independent of thermite compositions, the positive mass spectra all contain a strong Na peak, suggesting the positive ion species distributions are dominated by Na with minor species of Al and K for all the tested thermite systems. There is also a clear Bi peak ($m/z=209$) observed for Al/Bi_2O_3 thermite system, but no W species can be found for the case of Al/WO_3. This observation is consistent with the fact that Al/Bi_2O_3 produces the most intense ionization.

The mass spectrometric measurement indicates that the major current generating species are not the primary components comprising the composite particles, but rather Na and K derived salts that, while a minor component on a mass basis, evidently can result in intensive ion currents. The mass spectra patterns obtained for three different thermites show similar ion peak patterns, suggesting a common ionization mechanism that governs the generation of positive ion species.

D. On the mechanism of ion generation

Together with the observation of Al species in the mass spectra, we believe that the underlying ionization mechanism for positive ions should be closely related to the ion flux in the shell of the aluminum nanoparticles. Recently, we studied the ignition behavior of nanocomposite thermites under T-Jump heating conditions (heating rate $\sim 10^5$ K/s) and the results suggest that the ignition of nanocomposite thermites is controlled by diffusion of molten aluminum through the oxide shell.[27] Diffusion controlled metal oxidation theories have been studied for several decades and, depending on the types of metal or thickness of the oxide layer, various theoretical models have been developed to study metal oxidation.[28–30] It is believed that the diffusion of ions and electrons through the oxide shell due to concentration and pressure gradients, or an electric field within the oxide layer, is the controlling transport process for metal oxidation.[31–33] From Cabrera and Mott's[34] thin film growth theory, a strong electric field of the order of $\sim 10^7$ V/cm is predicted across the oxide shell caused by tunneling electrons, and thus ion transport is driven by the electric field.[35] We also observed a similar electric field driven ion transport in aluminum nanoparticles at high temperatures through molecular dynamics simulations.[21] The simulation results show that the strong electric field is intrinsically self-generated due to the presence of the oxide shell, which provides a strong driving force for ion transport. In the case of 6 nm aluminum nanoparticles with a 2 nm oxide shell, the simulations show an Al ion flux of ~ 20 mole/cm^2/s at 1100 K is primarily due to the electric field as opposed to the concentration and pressure gradients. For the larger aluminum nanoparticles that we used in these experiments, an even higher ion flux should be expected.

Based on the above discussion, the positive ion generation can be explained as follows. Prior to the ignition point the aluminum particles are already at elevated temperatures and the nascent electric field is formed across the oxide shell. Assisted by the electric field, aluminum ions move radially outward through the oxide shell. On the other hand, the salts exist at the particle surface in the form of Na^+, K^+, and Cl^- ions and are weakly bonded with surface atoms. As the aluminum ions reach the particle surface, electrostatic repulsion between Al^+ and Na^+ or K^+ eject the Na^+ and K^+ ions from particle surface. As a result, transient ion pulses composed of Na^+, K^+, and some Al^+ are observed just prior to the ignition of the thermites. If we assume the electrostatic repulsion force from a Coulomb potential only becomes significant when two ions are within 1 nm of each other, then, based on an Al ion flux of ~ 20 mole/cm^2/s predicted by our molecular dynamic simulations,[21] aluminum ions will be moving toward a single Na^+ or K^+ ion at the rate of $\sim 10^{11}$ number per second. In other words, during our observed ionization interval of ~ 0.1 ms, there are $\sim 10^7$ aluminum ions around a single Na^+ or K^+ ion. As a result of the strong electrostatic repulsion, Na^+ and K^+ ions are ejected as the most abundant species even though the salt contaminations in the thermite should be low. In addition, our experimental results suggest that the total number of positive ions produced from different thermite reaction systems are about the same regardless of the thermite compositions, consistent with a common source of ions regardless of particle type.

To test our diffusion based ion-current theory we mix the Al/Fe_2O_3 thermite sample with sodium chloride salt. As expected, the total positive ion signal in Fig. 7(a) shows the same transient nature of the ion generation but a much stronger intensity than regular Al/Fe_2O_3 thermite sample [Fig. 3(c)] and the corresponding mass spectra in Fig. 7(b) show strong Na, Al, and K peaks, agreeing with our expectation. The result shown in Fig. 7 confirms the salt contamination as the primary positive ions source and suggests that our diffusion flux based ionization mechanism for positive ion pulse generation is correct.

As our experimental results suggest, the ionization is a two step process, and the negative species are emitted during the ignition of thermite reactions. However, our current mass spectrometer configuration would not allow us to obtain negative mass spectra, and, consequently, it is difficult to extract complete mechanistic information without the knowledge of species identification. The fact that the negative ionization step occurs during the ignition event suggests the strong relation between the solid phase nanocomposite thermite reaction and the ionization process.

IV. CONCLUSIONS

During the development of the T-Jump/TOFMS for studying the nanocomposite thermite reactions, we observed a strong ion pulse generation phenomenon. In this paper we investigate the characteristic features of this ion pulse arising from the combustion of Al/CuO, Al/WO_3, Al/Fe_2O_3, and Al/Bi_2O_3 nanocomposite thermite mixtures. The transient current pulse nominally occurs over ~ 0.1 ms and is much shorter than the characteristic reaction time of typical thermite mixtures. The ion pulse signals for positive and negative species show that the thermite induced ionization occurs close to the point of ignition of the thermite powders and is characterized by two ionization steps. The first ionization

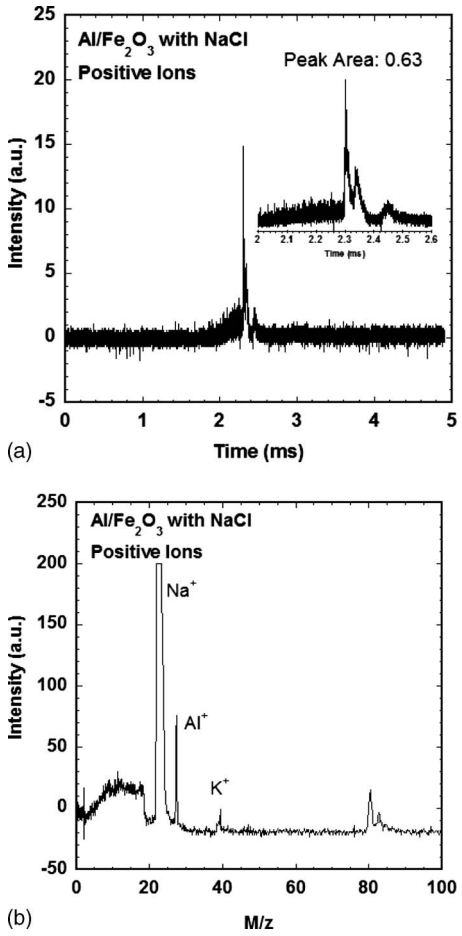

FIG. 7. (a) The total positive ion signal for a Al/Fe_2O_3 thermite sample mixed with sodium chloride salt and (b) the corresponding mass spectra measure of positive ion generated from the thermite reaction (without external electron impact ionization source).

step happens prior to ignition which primarily produces positive ions, and the ignition leads to a second ionization step which is dominated by negative species. The mass spectrometric measurements revealed that the positive ion species distributions are dominated by Na with minor species of Al and K for all the tested thermite systems. The positive ion generation was attributed to the interaction between the Al ion diffusion flux through the oxide shell and the salt contamination at the particle's surface. The strong electrostatic repulsion formed by the Al flux ejects the Na and K ions from the particle's surface. However, we are not able to obtain spectra for the negative species due to induced arcing from the strong negative ion pulse.

ACKNOWLEDGMENTS

We thank Dr. William Fourney for the use of his high speed camera system. We also gratefully acknowledge the financial support from the Army Research Office, the Defense Threat Reduction Agency, and the Office of Naval Research.

[1]K. Sullivan, G. Young, and M. R. Zachariah, Combust. Flame **156**, 302 (2009).
[2]S. M. Umbrajkar, S. Seshadri, M. Schoenitz, V. K. Hoffmann, and E. L. Dreizin, J. Propul. Power **24**, 192 (2008).
[3]A. Prakash, A. V. McCormick, and M. R. Zachariah, Nano Lett. **5**, 1357 (2005).
[4]L. Zhou, N. Piekiel, S. Chowdhury, and M. R. Zachariah, Rapid Commun. Mass Spectrom. **23**, 194 (2009).
[5]G. Young, K. Sullivan, and M. R. Zachariah, Combust. Flame **156**, 322 (2009).
[6]V. E. Sanders, B. W. Asay, T. J. Foley, B. C. Tappan, A. N. Pacheco, and S. F. Son, J. Propul. Power **23**, 707 (2007).
[7]M. L. Pantoya and J. J. Granier, J. Therm. Anal. Calorim. **85**, 37 (2006).
[8]M. A. Trunov, M. Schoenitz, and E. L. Dreizin, Propellants, Explos., Pyrotech. **30**, 36 (2005).
[9]K. B. Plantier, M. L. Pantoya, and A. E. Gash, Combust. Flame **140**, 299 (2005).
[10]A. B. Fialkov, Prog. Energy Combust. Sci. **23**, 399 (1997).
[11]I. A. Filimonov and N. I. Kidin, Shock Waves **41**, 639 (2005).
[12]A. P. Ershov, Combust., Explos. Shock Waves **11**, 798 (1975).
[13]M. Setoodeh, K. S. Martirosyan, and D. Lussa, J. Appl. Phys. **99**, 084901 (2006).
[14]K. S. Martirosyan, M. Setoodeh, and D. Luss, J. Appl. Phys. **98**, 054901 (2005).
[15]A. I. Kirdyashkin, V. L. Polyakov, Y. M. Maksimov, and V. S. Korogodov, Combust., Explos. Shock Waves **40**, 180 (2004).
[16]K. S. Martirosyan, J. R. Claycomb, J. H. Miller, Jr., and D. Luss, J. Appl. Phys. **96**, 4632 (2004).
[17]D. L. Igor Filimonov, AIChE J. **50**, 2287 (2004).
[18]K. S. Martirosyan, J. R. Claycomb, G. Gogoshin, R. A. Yarbrough, J. H. Miller, and D. Luss, J. Appl. Phys. **93**, 9329 (2003).
[19]K. S. Martirosyan, I. A. Filimonov, and D. Luss, Int. J. Self-Propag. High-Temp. Synth. **12**, 91 (2003).
[20]K. S. Martirosyan, I. A. Filimonov, M. D. Nersesyan, and D. Luss, J. Electrochem. Soc. **150**, J9 (2003).
[21]B. J. Henz, T. Hawa, and M. R. Zachariah, "On the role of built-in electric fields on oxidation of oxide coated nanoaluminum: Ion mobility versus Fickian diffusion," J. Appl. Phys. (in press).
[22]Z. A. Munir, Mater. Sci. Eng., A **287**, 125 (2000).
[23]F. B. Carleton and F. J. Weinberg, Nature (London) **330**, 635 (1987).
[24]D. G. Tasker, B. W. Asay, J. C. King, V. E. Sanders, and S. F. Son, J. Appl. Phys. **99**, 023705 (2006).
[25]V. S. Korogodov, A. I. Kirdyashkin, Y. M. Maksimov, A. A. Trunov, and R. M. Gabbasov, Combust., Explos. Shock Waves **41**, 481 (2005).
[26]L. Zhou, N. Piekiel, S. Chowdhury, and M. R. Zachariah (in preparation).
[27]S. Chowdhury, K. Sullivan, N. Piekiel, L. Zhou, and M. R. Zachariah, J. Phys. Chem. C (submitted).
[28]A. Atkinson, Rev. Mod. Phys. **57**, 437 (1985).
[29]A. T. Fromhold, Jr., *Theory of Metal Oxidation* (North-Holland, Amsterdam, 1980), Vol. 2.
[30]A. T. Fromhold, Jr., *Theory of Metal Oxidation* (North-Holland, Amsterdam, 1976), Vol. 1.
[31]A. Rai, K. Park, L. Zhou, and M. R. Zachariah, Combust. Theory Modell. **10**, 843 (2006).
[32]A. T. Fromhold and E. L. Cook, Phys. Rev. **175**, 877 (1968).
[33]C. Wagner, Z. Phys. Chem. Abt. B **21**, 25 (1933).
[34]N. Cabrera and N. F. Mott, Rep. Prog. Phys. **12**, 163 (1948).
[35]V. P. Zhdanov and B. Kasemo, Chem. Phys. Lett. **452**, 285 (2008).